

---

# COMPUTATIONAL GRAPH REPRESENTATION OF EQUATIONS SYSTEM CONSTRUCTORS IN HIERARCHICAL CIRCUIT SIMULATION

---

Zichao Long   Lin Li   Lei Han   Xianglong Meng   Chongjun Ding   Ruiyan Li   Wu Jiang

Fuchen Ding   Jiaqing Yue   Zhichao Li   Yisheng Hu   Ding Li   Heng Liao \*

HiSilicon

## ABSTRACT

Equations system constructors of hierarchical circuits play a central role in device modeling, nonlinear equations solving, and circuit design automation. However, existing constructors present limitations in applications to different extents. For example, the costs of developing and reusing device models — especially coarse-grained equivalent models of circuit modules — remain high while parameter sensitivity analysis is complex and inefficient. Inspired by differentiable programming and leveraging the ecosystem benefits of open-source software, we propose an equations system constructor using the computational graph representation, along with its JSON format netlist, to address these limitations. This representation allows for runtime dependencies between signals and subcircuit/device parameters. The proposed method streamlines the model development process and facilitates end-to-end computation of gradients of equations remainders with respect to parameters. This paper discusses in detail the overarching concept of hierarchical subcircuit/device decomposition and nested invocation by drawing parallels to functions in programming languages, and introduces rules for parameters passing and gradient propagation across hierarchical circuit modules. The presented numerical examples, including (1) an uncoupled CMOS model representation using "equivalent circuit decomposition+dynamic parameters" and (2) operational amplifier (OpAmp) auto device sizing, have demonstrated that the proposed method supports circuit simulation and design and particularly subcircuit modeling with improved efficiency, simplicity, and decoupling compared to existing techniques.

---

\*Corresponding author

# Contents

<b>1</b>	<b>Introduction</b>	<b>3</b>
<b>2</b>	<b>Hierarchical Circuit Equations System Constructor: Computational Graph</b>	<b>4</b>
2.1	Subcircuit Module Definition in JSON Format Netlist . . . . .	5
2.2	Representation of Subcircuit Module Instances in a Program . . . . .	6
2.3	Instance Compilation from Subcircuit Module Definition . . . . .	7
	Basic Elements . . . . .	7
2.4	Execution: Forward and Backward Pass of a Computational Graph . . . . .	8
	SubModel and Internal Parameters . . . . .	8
	Layer-wise Gradient Backpropagation . . . . .	9
<b>3</b>	<b>Applications</b>	<b>10</b>
3.1	CMOS Device Model: Equivalent Circuit Decomposition + Dynamic Parameters . . . . .	10
3.2	OpAmp Device Sizing: DC Operating Points Optimization Under Different PVT Combinations . . . . .	11
<b>4</b>	<b>Conclusion</b>	<b>13</b>
	<b>Acknowledgment</b>	<b>13</b>
	<b>References</b>	<b>13</b>
	<b>Appendix</b>	<b>16</b>
A	TRAN Analysis Induced AC Analysis Equation . . . . .	16
B	CMOS Subcircuit . . . . .	16
C	Gradient Backpropagation of the Solution of a Linear Equations System . . . . .	17

# 1 Introduction

Analog circuit simulation (Figure 1) [1–3] has become one of the most important tools in the analog circuit EDA toolchain to assist verification and design. This is due to long-term research accumulation in algebraic differential equation theory [4–6], device modeling [7–9], equations system construction [10–12], nonlinear equations solvers [13, 14], hardware description languages (HDLs) [15–19], and more. However, we still see inconveniences with popular

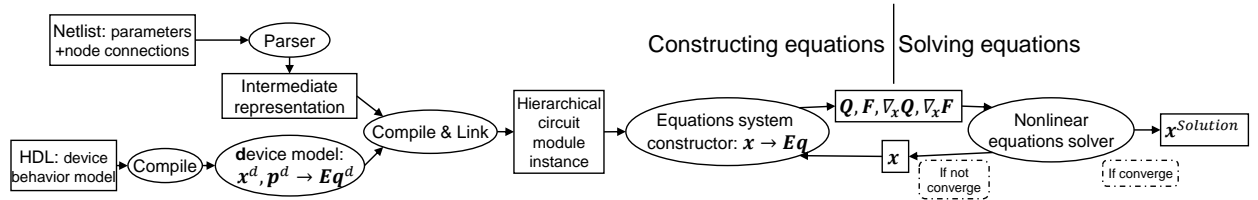


Figure 1: Simulator flowchart

HDLs and simulators in reusing coarse-grained circuit module behavior models, introducing multi-physical effects, and applying gradient optimization methods to automatic design.

- For device and circuit modeling, HDL technology is often used to create a device behavior model, which is then compiled [17] into a program that the simulator can invoke. In particular, multi-port circuit behavior modeling often goes through two steps: function fitting and HDL implementation, for example, neural network fitting [20, 21]+HDL or Volterra polynomial [22]+SPICE netlists [23, 24].
- To achieve an optimal combination of circuit parameters in the automation of analog circuit design [25–27], it is necessary to first optimize the device size. Prior to 2010, researchers developed solutions based on gradient optimization using parameter sensitivity analysis [28, 29]. To tune design variables, modern process and software technologies require that software uses callbacks to modify model parameters. However, such an approach hinders users from obtaining gradient information of the variables. This has pushed recent research to shift its focus toward black-box methods, such as local sampling for gradient reconstruction [30–32], surrogate models [33–36], and reinforcement learning [37].

Many works attempt to address the above inconveniences from both the model compilation and the gradient acquisition perspectives. For example, Mahmutoglu et al. [38] developed the Verilog-AMS compiler that can run using Matlab/Octave, Kuthe et al. [39] can obtain more information about the equations and internal derivatives when the Verilog-AMS circuit module is compiled, and Hu et al. [40] provides an efficient implementation of adjoint equations for transient simulation. However, none of these works explore functional support possibilities from the perspective of systems equations construction.

Indeed, one significant cause of these inconveniences is that the analog HDLs contain many complex and even bloated features, which are necessary for these HDLs to simultaneously support the representation of structural and behavioral information. Such features include the automatic differentiation required for analog simulation, and polynomial interpolation that may be used in modeling [15, Sections 4.5.6, 9.21]. The intertwining of structural and behavioral information has isolated analog HDLs from the open ecosystems of other programming languages and tools, and also created high barriers for developing analog EDA tools. Furthermore, only static circuit parameters independent of signal values can be passed between nested circuit modules and simulation runtime variables are allowed only within modules ([15, Sections 3.4, 6],[16, Section 4.10]) — this is not conducive to reuse and development of coarse-grained circuit models.

Thriving technologies such as deep learning [41] and automatic differential programming [42] have contributed to a number of research fields in scientific computing, including data-driven multi-scale modeling and inverse problems [43–45]. Inspired by such works, this paper proposes a computational graph implementation of an equations system constructor that works in hierarchical circuit simulation [12, 46–48], along with the corresponding JSON netlist and compilation method (Figure 2). The internal and external variables, design variables, model input parameters, and corresponding gradients of circuit modules are processed in a unified manner. This work takes circuit modules as the basic units of a computational graph and supports decoupled representation of circuit models using "equivalent circuit decomposition using JSON netlist+submodel for computing dynamic parameters". The advantages of this approach are twofold: (1) JSON format is easy to parse, and its basic data types "dictionary+list" are sufficient to represent circuit structure information. And (2), a submodel can be implemented with the help of the automatic differentiation capability of Julia[49]. Based on these two advantages, the proposed method in this paper simplifies circuit modeling and enhances the gradient acquisition capability of simulation tools.

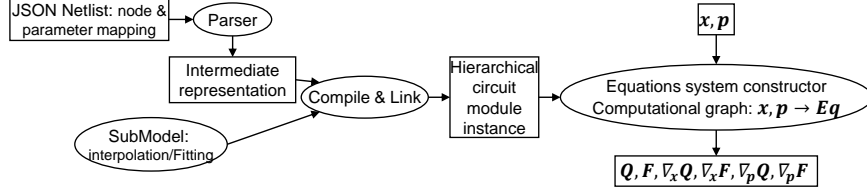


Figure 2: Flowchart: create computational graph from a JSON netlist

Section 2 describes the processing of structural information related to circuit modules in a computational graph. Similar to defining, compiling, representing, and executing functions in a programming language [50–52], the process involves the following steps: module definition (netlist), parsing and compilation, data structures of module instances, and graph executor (Figure 3). Additionally, Section 2.4 introduces how to define and use SubModel for computing intrinsic dynamic parameters to provide behavioral information of each circuit module. Section 3 presents two application examples, one for device modeling and the other for a joint solution of DC/AC analysis and device sizing under different process, voltage, and temperature (PVT) combinations.

## 2 Hierarchical Circuit Equations System Constructor: Computational Graph

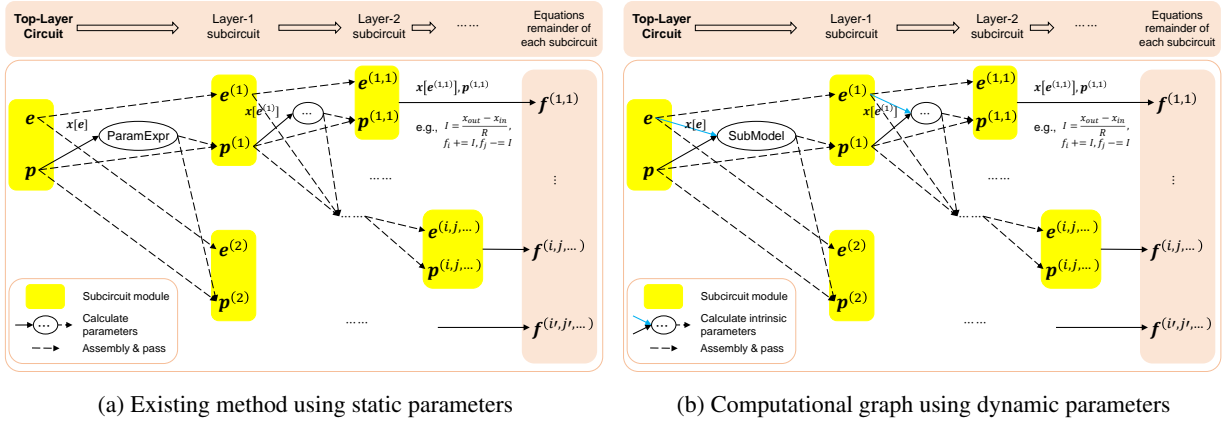


Figure 3: Equations system constructor for hierarchical circuits: existing method v.s. computational graph. Each computing unit corresponds to a subcircuit, which can be decomposed into smaller subcircuits — the smallest granularity subcircuit are the "basic elements".  $e^{(\dots)}$  denotes the internal and external nodes of a subcircuit,  $x$  a generalized signal, such as node bias or branch current,  $p^{(\dots)}$  the input parameters of a subcircuit, for example, the device size (alternatively, a non-linear capacitance, inductance, or current value of a basic element, functioning as a dynamic parameter), and  $f^{(\dots)}$  the contribution of a subcircuit to the remainder of the simulation equations. Calculation of the Jacobian matrix is omitted in this schematic. In the existing method, a lower-layer parameter of a circuit module does not depend on the signal value ( $x[e]$ ), and calculation of ParamExpr can be completed when the netlist is built. In the computational graph method, the dynamic parameters are derived from the [intrinsic parameters](#) output by SubModel — these parameters are obtained at the calculation runtime of the systems of equations.

For any  $N$  generalized signals (i.e., equation unknowns)  $x \in \mathbb{R}^N$  and  $M$  signal-independent input variables or parameters  $p \in \mathbb{R}^M$ , the mathematical meaning of circuit simulation is constructing and solving the following conservation algebraic differential equations [6, 14, 40]

$$f(\dot{x}(t), x(t), p) \triangleq \frac{dQ(x, p)}{dt} + F(x, p) = 0, \quad (\text{Eq (Flat)})$$

where,  $Q$  denotes the dynamic part of the remainder of the equation (e.g., the charge of different capacitors and magnetic flux of different inductors) and  $F$  denotes the static part of the remainder of the equation (e.g., the total input DC current at each node and the voltage drop equation). Modern simulators tend to decompose and construct Eq (Flat) based on

circuit hierarchy, which are easier to understand and parallelize:

$$\begin{aligned} \mathbf{f}(\hat{\mathbf{x}}, \mathbf{x}, \mathbf{p}) &= \mathbf{f}^{(1)}(\hat{\mathbf{x}}^{(1)}, \mathbf{x}^{(1)}, \mathbf{p}^{(1)}) + \mathbf{f}^{(2)}(\hat{\mathbf{x}}^{(2)}, \mathbf{x}^{(2)}, \mathbf{p}^{(2)}) + \dots \\ &= \mathbf{f}^{(1,1)} + \mathbf{f}^{(1,2)} + \dots + \mathbf{f}^{(2,1)} + \mathbf{f}^{(2,2)} + \dots, \end{aligned} \quad (\text{Eq (Hierarchical)})$$

where,  $\mathbf{x}^{(i)}$ ,  $\mathbf{p}^{(i)}$ , and  $\mathbf{f}^{(i)}$  respectively denote the input signals, parameters or variables, and contribution to the remainder of the equation of subcircuit  $i$  of the given circuit. The overlapping part between  $\mathbf{x}^{(i)}$  and  $\mathbf{f}^{(i)}$  depends on the common nodes of the subcircuits. As shown in Eq (Hierarchical),  $\mathbf{f}^{(i)}$  may be further decomposed into  $\mathbf{f}^{(i,1)}$ ,  $\mathbf{f}^{(i,2)}$ ,  $\dots$  as required.

Note that Eq (Flat) represents only transient (TRAN) equations, and Eq (Flat) is usually discretized in the time direction during numerical solution. At each time step, the system of algebraic equations is solved using the Newton-Raphson method [12, Section 7.1]

$$\text{Solve } \mathbf{x}, \text{ Subject to } \frac{1}{\beta \Delta t} \mathbf{Q}(\mathbf{x}, \mathbf{p}) + \mathbf{F}(\mathbf{x}, \mathbf{p}) + \mathbf{b} = \mathbf{0},$$

where  $\mathbf{Q}$ ,  $\mathbf{F}$ , and sparse Jacobian matrix  $\nabla_{\mathbf{x}} \mathbf{Q}$ ,  $\nabla_{\mathbf{x}} \mathbf{F}$  need to be repeatedly calculated. For other types of simulation such as DC analysis and AC small signal analysis, Eq (Flat) must be converted (Appendix A). Because the processing of each analysis equation is similar, the following uses TRAN analysis and a simple JSON netlist subcircuit definition (Code 1) as an example to describe how to denote the calculation of  $\mathbf{Q}^{(\dots)}$ ,  $\mathbf{F}^{(\dots)}$ ,  $\nabla_{\mathbf{x}^{(\dots)}} \mathbf{Q}^{(\dots)}$  or  $\nabla_{\mathbf{p}^{(\dots)}} \mathbf{Q}^{(\dots)}$ , and  $\nabla_{\mathbf{x}^{(\dots)}} \mathbf{F}^{(\dots)}$  or  $\nabla_{\mathbf{p}^{(\dots)}} \mathbf{F}^{(\dots)}$  in hierarchical circuit simulation as the forward and backward pass of a computational graph (Figure 3b).

## 2.1 Subcircuit Module Definition in JSON Format Netlist

Similar to Verilog-AMS [15, Section 6], we define a circuit module that contains five parts of information (Table 1): (1) external nodes; (2) internal nodes; (3) input parameters; (4) decomposition of internal subcircuits; and (5) intrinsic parameters.

Listing 1: User-defined subcircuit named SizeDepResistor in the netlist: a resistor whose resistance is size-dependent

```
"SizeDepResistor":{ # Define the subcircuit module.
  "ExternalNodes":["l","r"],
  "InputParams":["Rlength","Rwidth"],
  "InternalNodes":[],
  "SubModel":{
    "Expr":["1e2*Rlength/Rwidth, "],
    "IntrinsicParams":["RValue"]
  },
  "Schematic":{
    # Instantiate each subcircuit or element in the module.
    "instanceR":{
      "MasterName":"resistor",
      "ExternalNodes":{"left":"l","right":"r"},
      "InputParams":{"resistance":"RValue"}
    }
  }
}
```

Table 1: Subcircuit module definition

	Content	Field	
Structural information (dictionary+list)	List of external node names	ExternalNodes	Required
	List of internal node names	InternalNodes	Required
	List of input parameter names	InputParams	Required
	Internal subcircuit decomposition	Schematic	Required
Behavioral information (differentiable function)	Submodel for calculating intrinsic parameters	SubModel	Optional

The "Schematic" field represents internal subcircuit decomposition, which includes zero or more instantiation statements of subcircuits/devices. Each instantiation statement in "Schematic" is composed of (1) an instance name; (2) a class

name (or master name); (3) external node connections; and (4) input parameter values. Code 1 provides an example, where the subcircuit decomposition part involves only one instance.

- "instanceR" indicates the instance name.
- "MasterName" indicates that the instance is of the "resistor" class. The class, or master, can be a subcircuit module or a type of built-in supported basic element.
- "ExternalNodes" indicates that the two external nodes "left" and "right" of the instance are respectively connected to ports "l" and "r" of the module, i.e., "SizeDepResistor" here. In general case, the nodes connected to each instance in "Schematic" must come from "ExternalNodes" and "InternalNodes" of the given module.
- "InputParams" indicates that the parameter of the instance is the internal variable "RValue" calculated by "SubModel". The parameters referenced by the instance in "Schematic" must come from: (1) global variables; (2) "InputParams" of the module; (3) "IntrinsicParams" under "SubModel" (if any) of the model.

For more information about SubModel and its functionality, see Section 2.4.

## 2.2 Representation of Subcircuit Module Instances in a Program

The subcircuit definition should be compiled into an appropriate hierarchical data structure (Figure 4) so that the equations system constructor can efficiently invoke subcircuit modules. A compiled subcircuit module contains two parts: common computation rules of subcircuits of the same master (Table 3) and instance private data (Table 2) There

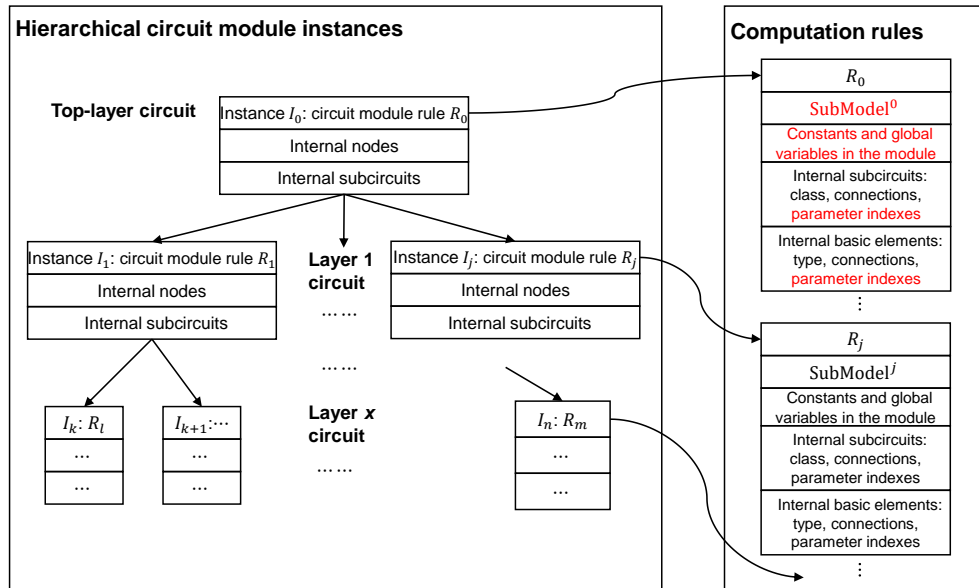


Figure 4: Schematic diagram of hierarchical subcircuit module instances and computation rules. Text in red indicates the parts that mark the differences from the existing method [48]. Because the existing method does not need to support dynamic parameters, it is only necessary to store the fixed parameters of the devices in the computation rules of each circuit module. However, because the proposed method requires that parameters passed to lower-layer instances and devices be calculated during runtime, parameter indexing is necessary.

Table 2: Instance private data of a subcircuit module

Symbol	Description
rule	Pointer to the corresponding computation rules (Table 3)
in	Internal nodes
subckts	Pointers to lower-layer subcircuit instances

are a few points to note:

1. The external nodes of a subcircuit are from its upper-layer subcircuits. The top-layer circuit is a closed system without external nodes.

Table 3: Computation rule of a subcircuit module

Symbol	Description
<b>c</b>	Constants
<b>gv</b>	Global variables
SubModel	SubModel for calculating intrinsic parameters
SubCktsInfo	Lower-layer subcircuit nodes and parameter indexes
BasicElementInfo	Basic element nodes and parameter indexes

2. Subcircuit instances may share external nodes with one another, but the internal nodes of a subcircuit instance are exclusive to itself. When instantiating a subcircuit, ensure that its internal nodes do not conflict with each other.
3. Global variables and system signals  $x$  are globally visible to all subcircuit modules. Only the indexes **gv** of global variables need to be stored in the module's computation rules (Table 3). The internal and external nodes of a module are also indexed for easy storage and passing.
4. If interactive analysis and debugging require more support information, the subcircuit master names, internal and external node parameter names, and lower-layer subcircuit instantiation statements can be added to a computation rule (Table 3). Additionally, the input parameters can be dynamically recorded in an instance (Table 2).

### 2.3 Instance Compilation from Subcircuit Module Definition

A JSON netlist file can be parsed using JSON parser tools available in a variety of programming languages. The compilation of the subcircuit module definition (Section 2.1) involves two steps:

1. Compile the computation rules of all subcircuit modules (Figure 5a). SubModel finishes parsing and compilation based on the compiler's implementation. To process other structural information (i.e., to create nodes and parameters indexes), only basic algorithms and data structures such as lists and dictionaries are needed.
2. Recursively instantiate the hierarchical circuit modules (Figure 5b). The indexes of the input nodes are offset by  $n = 0$  if the instantiation program was launched at top layer circuit. The proposed method ensures that the internal nodes of each subcircuit module are independent of each other.

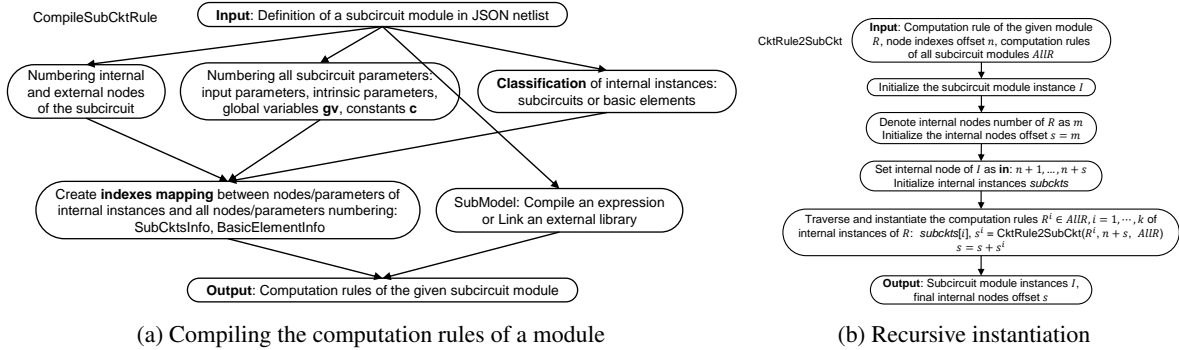


Figure 5: Compiling circuit modules

Note that the internal subcircuit decomposition of a circuit module may include both basic elements and other circuit modules defined in the netlist. As such, the compiler should be able to distinguish between these two types of instances before it creates indexes for nodes and parameters. This is in addition to the compiler being able to check that there are no circular definitions of subcircuit class, undefined subcircuit modules, disconnected subcircuits, and unused nodes in the circuit.

**Basic Elements** Basic elements are the smallest grained subcircuits without internal nodes or devices. Table 4 provides a brief list of supported basic elements. To add a type of basic elements, we need to define the electrical response function for each analysis and then provide information such as external nodes and input parameters to the compiler.

According to the modified nodal analysis method [11], the basic elements of the voltage source type must take the branch current as one of the degrees of freedom — this branch current is processed as an external GALV node in

Table 4: Supported basic elements

MasterName	ExternalNodes	InputParams	Remarks
resistor	left,right	resistance	Resistor
capacitor	input,output	capacitance	Capacitor
inductor	input,output	inductance	Inductor
CS	input,output	current	Current Source
VS	input,output	voltage	Voltage Source
VCCS	left,right,input,output	MF	Voltage Controlled Current Source
CCCS	iorigin,input,output	MF	Current Controlled Current Source
VCVS	left,right,input,output	MF	Voltage Controlled Voltage Source
CCVS	iorigin,input,output	MF	Current Controlled Voltage Source

the compiler. At compile time, the GALV node needs to be added to the upper-layer module as an internal node. A generalized external GALV node can also be added for basic elements of a non-voltage source type such as resistors, to indicate the current flowing through the element branch. Consider a TRAN analysis example, with the resistance of the resistor denoted as  $R$ , the left and right nodes  $l$  and  $r$ , the voltage value  $x_l$  and  $x_r$ , and with or without the GALV node and current value  $i$ ,  $x_i$ , we can present the remainder of the equation corresponding to the resistor using a sparse vector as follows:

$$\text{Without external GALV: } \mathbf{Q} = \mathbf{0}, \mathbf{F} = [(l, -\frac{x_l-x_r}{R}), (r, \frac{x_l-x_r}{R})]$$

$$\text{With external GALV: } \mathbf{Q} = \mathbf{0}, \mathbf{F} = [(l, -x_i), (r, x_i), (i, x_r - x_l + R \cdot x_i)]$$

The two equations correspond to the so-called "element stamps" of the same type of elements described in [14, Section 2.4.4]. We may also consider them as two network analysis methods [10, 11] for the same type of elements, which requires the support of both the compiler and the equations system constructor. For different analysis type, the calculation of remainder terms and that of the gradients in the basic element simulation equation must be distinguished — we will not discuss that in detail here.

## 2.4 Execution: Forward and Backward Pass of a Computational Graph

Each basic computing unit of the computational graph (Figure 3b) corresponds to a subcircuit instance. When the subcircuit is invoked in a computational graph, the computing unit first takes external nodes and input variables as input from upper layer circuit. The compute unit then traverses the internal subcircuit and basic devices to calculate the equation remainder and the signal and variable gradients. Finally, these results are returned to the upper layer. See Algorithm 1 for the internal process details.

Figure 6 shows steps 1 to 5 of Algorithm 1, where **en**, **ip**, **in**, **gv**, and **intrap** stand for external nodes, input parameters, internal nodes, global variables, and intrinsic parameters, respectively. The internal and external nodes **en**, **in** of the circuit may be used to index the generalized signal values  $\mathbf{x}[\mathbf{en}]$ ,  $\mathbf{x}[\mathbf{in}]$ , respectively. The variables/parameters  $\mathbf{p}$  involved in the circuit module consists of four parts: **ip**, **gv**, **intrap**, and **c**.

**SubModel and Intrinsic Parameters** In the computational graph, SubModel takes the internal and external signals and input parameters of the module as inputs, and outputs all *intrinsic parameters* via **intrap**=SubModel(**signals**,**ip**), where **nodes**=[**en**,**in**], **signals**= $\mathbf{x}[\mathbf{nodes}]$ , which can be passed to the lower-layer subcircuits and basic elements. This setup is based on the Assumption 1: "The behavior of a circuit module is and only is determined by the internal and external signals as well as input variables." Thus, for a SubModel, there is no need to perceive the internal signals of lower-layer subcircuits nor the node signals or parameters of other irrelevant modules. This setting can cover a considerably wide range of nonlinear effects and is easy to program.

**Assumption 1.** *The intrinsic parameters in a subcircuit module are uniquely determined by the bias signals of the internal and external nodes and the input parameters of the module.*

The submodel in the circuit definition should provide sufficient information so that the compiler can register the SubModel with the common rules (Table 3). In addition, there should be some protocol between the computational graph and the SubModel for obtaining the Jacobian matrix of **intrap** with respect to **signals**,**ip**

$$J_s = \nabla_{\mathbf{signals}} \mathbf{intrap}, J_{ip} = \nabla_{\mathbf{ip}} \mathbf{intrap}, \quad (1)$$

The specific implementation depends on the programming language used. As such, details are not provided here.



**Algorithm 1:** Calling a Subcircuit

equations remainder, signal gradient, variable gradient =  
 EvalCompositeSubCkt( $x$ , ckt, en, ip)

Input: System signals  $x$ , subcircuit instance ckt, external node indexes **en**, input parameters **ip**;

# Internal information of ckt: Internal nodes **in**, SubModel, global variables **gv**, constants **c**;

1. Assemble the internal nodes **in** and external nodes **en** of ckt, resulting in **nodes**=[**en**,**in**];

2. Calculate the intrinsic parameters according to the internal and external signals and input parameters: **intrp** = SubModel( $x$ [**nodes**], **ip**);

3. Assemble all variables and parameters of ckt, resulting in **params**= [**ip**, **intrp**, **gv**, **c**];

4. Extract the external nodes **suben**  $\subset$  **nodes** and input parameters **subip**  $\subset$  **params** of each subcircuit (subckt) in ckt from **nodes**, **params**, and call EvalCompositeSubCkt( $x$ , subckt, **suben**, **subip**);

5. Extract the external nodes and input parameters of each basic element in ckt from **nodes**, **params**, and calculate the equation remainder and gradient of each basic element;

6. Collect the remainder terms of all equations in steps 4 and 5;

7. Propagate signal and variable gradients of lower-layer subcircuits and basic elements backward according to the index mapping of steps 1 to 5;

Output: Equation remainder, signal gradient, variable gradient

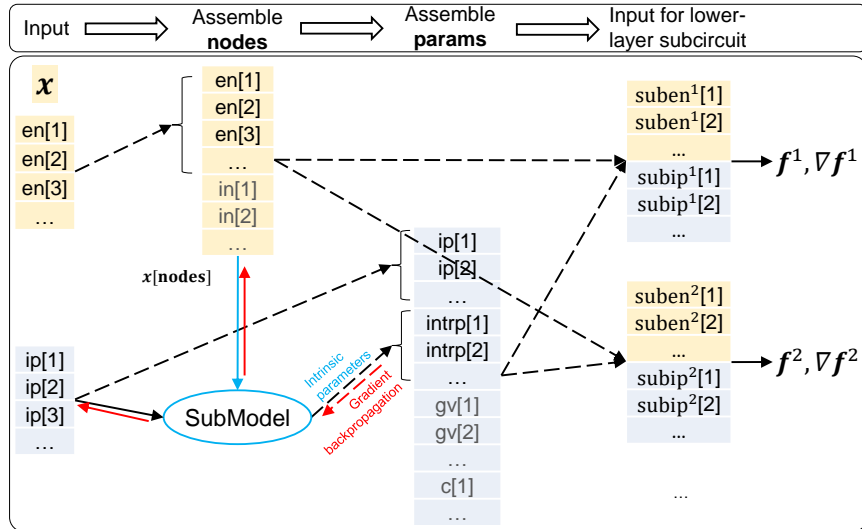


Figure 6: Schematic diagram of steps 1 to 5 of Algorithm 1, also a zoom-in view of the calls to the top-layer to layer-1 subcircuits in Figure 3b. In the existing method, the input and intrinsic parameters are computed at compile time, and no gradient of parameters are propagated backward at runtime.

**Layer-wise Gradient Backpropagation** A computational graph completes the computation process by calling subcircuits. The computing logic differs from that involved in the existing method (Figure 3) in one major aspect: In the computational graph, the input parameters **subip** of lower-layer modules or elements come from a subset of the assembled parameters **params** (Figure 6). Consequently, gradient backpropagation for **subip** is required. The following describes the gradient backpropagation process in Algorithm 1 for TRAN simulation as an example.

For TRAN analysis, the returned value of Algorithm 1 contains the following eight items:  $Q, F, \nabla_x Q, \nabla_x F, \nabla_{gv} Q, \nabla_{ip} Q, \nabla_{gv} F$ , and  $\nabla_{ip} F$ . Because the gradient backpropagation of  $Q$  is the same as that of  $F$ , only  $Q$  is considered for simplicity. The computation results of all subcircuits of Algorithm 1 are recorded as  $\{Q^i\}$ ,  $\{\nabla_x Q^i\}$ ,  $\{\nabla_{gv} Q^i\}$ , and  $\{\nabla_{subip^i} Q^i\}$ , where the superscript  $i$  denotes the sequence number of the internal subcircuit or basic element.  $Q^i, \nabla_x Q^i$ , and  $\nabla_{gv} Q^i$  can be directly assembled as

$$Q = \sum_i Q^i, \nabla_x Q = \sum_i \nabla_x Q^i, \nabla_{gv} Q = \sum_i \nabla_{gv} Q^i,$$

while the gradient backpropagation of  $\nabla_{subip^i} Q^i$  needs to be processed differently based on the index of **subip** <sup>$i$</sup>  to **params**=[**ip**,**intrp**,**gv**,**c**].

1. If  $\text{subip}^i[j] \in \mathbf{c}$ , backpropagation is not performed.
2. If  $\text{subip}^i[j] \in \mathbf{ip} \cup \mathbf{gv}$ , then  $\nabla_{\text{subip}^i[j]} Q^i$  is propagated to the corresponding  $\nabla_{\mathbf{ip}} Q$  or  $\nabla_{\mathbf{gv}} Q$ .
3. If  $\text{subip}^i[j] = \mathbf{intrp}[l]$  for any index  $l$  (Figure 6), given Assumption 1 and the Jacobian matrix of the intrinsic parameters with respect to the signal and input parameters (Equation 1), then (let  $\mathbf{g} \triangleq \nabla_{\text{subip}^i[j]} Q^i$ )

$$\nabla_{x[\text{nodes}]} Q += J_s[:, l] \otimes \mathbf{g}, \nabla_{\mathbf{ip}} Q += J_{\mathbf{ip}}[:, l] \otimes \mathbf{g}. \quad (2)$$

where,  $\otimes$  represents the outer product of two vectors.

### 3 Applications

#### 3.1 CMOS Device Model: Equivalent Circuit Decomposition + Dynamic Parameters

As mentioned earlier, any subcircuit module (e.g., CMOS) that satisfies Assumption 1 can be modeled as a submodel-based representation featuring "equivalent circuit decomposition + dynamic parameters". This section provides an implementation example based on a lookup table. Reimplementing BSIM model [7] as a SubModel is a conventional method that offers better compatibility with the existing method, but it is not adopted in this work. The CMOS module definition consists of the following elements (details about the definition are provided in Appendix B and the equivalent circuit diagram under AC analysis is given in Figure 7):

1. Internal and external nodes: **nodes**=[gate,source,drain,bulk];
2. Input parameters for the device size: **ip**=[MosL,MosW];
3. Intrinsic parameters output by SubModel: **intrp**=[ID,GDS,CDD,CSS,CGG,CGS,CGD, GM,GMB], whose value is determined by the four bias voltage values (**nodes**) and device size (**ip**).

The compiler loads external libraries and generates a function object of class "lut.MosLookup" to register it as a submodel in the subcircuit rule (Table 3). Among the intrinsic parameters, ID indicates the DC current between source and drain under DC analysis, and GDS, CDD, GM, etc. are equivalent small-signal parameters under AC analysis. There are a few points to note:

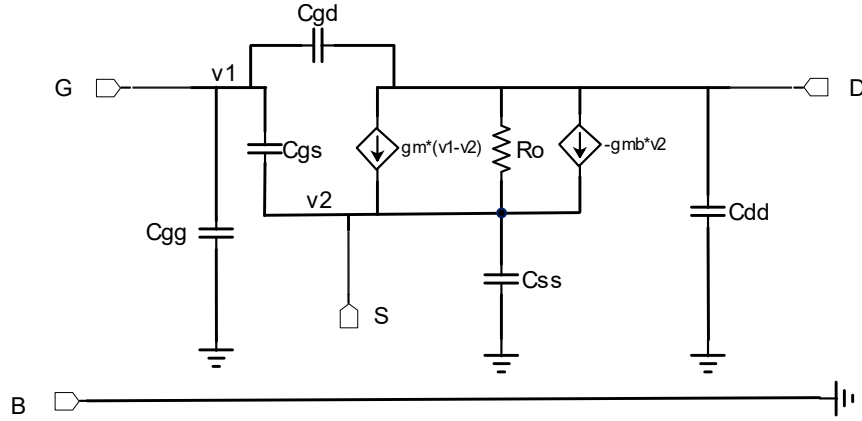


Figure 7: CMOS equivalent small-signal model [25, Figure 2.39], where,  $R_o$  is a resistor with resistance  $\frac{1}{GDS}$ .

1. The role of built-in basic elements ICS and ACVCCS (Appendix B) is to ensure that ID only functions under DC analysis, while GDS, GM and GMB only function under AC analysis.
2. The DCAC hybrid analysis or DC analysis computational graph of the equation constructor can execute this circuit module. However, the pure AC analysis computational graph cannot independently run this circuit module: In order to establish the AC analysis equations, it is necessary to first compute [GDS,GM], etc., which are determined by the DC bias voltage. This is different from directly inducing small signal linear equations through TRAN analysis equations (Appendix A). In fact, Assumption 1 also stipulates that internal variables can depend on the bias voltage signal, but not on the small signals in linear analysis.
3. The SubModel can freely call external programs, such as using three-dimensional spline interpolation, provided that it ensures compliance with the interface requirements of the corresponding automatic differentiation system.

This submodel-based device model representation method features "equivalent circuit decomposition + dynamic parameters" and shows the following advantages:

1. Decoupled from circuit network analysis or simulation, the submodel is only responsible for calculating the intrinsic parameters and Jacobian matrix (Section 2.2). Circuit connectivity is not the submodel's concern.
2. The syntax and capability boundary of a submodel in calculating intrinsic parameters depend on the compiler's processing of the "SubModel" field in the netlist. This can be implemented easily using various external programs and automatic differential tools.

### 3.2 OpAmp Device Sizing: DC Operating Points Optimization Under Different PVT Combinations

Figure 8 shows the device sizing process in analog circuit design. Specifically, designers connect available devices accessible to the target process into circuits, and adjust the size of each device (such as a CMOS device) based on specific methodologies and experience so that a circuit can fulfill specification requirements under a given area and power consumption constraints. In this process, repeated circuit simulation is done to quantitatively inspect the behavior and performance of a circuit without the need to manufacture the physical circuit.

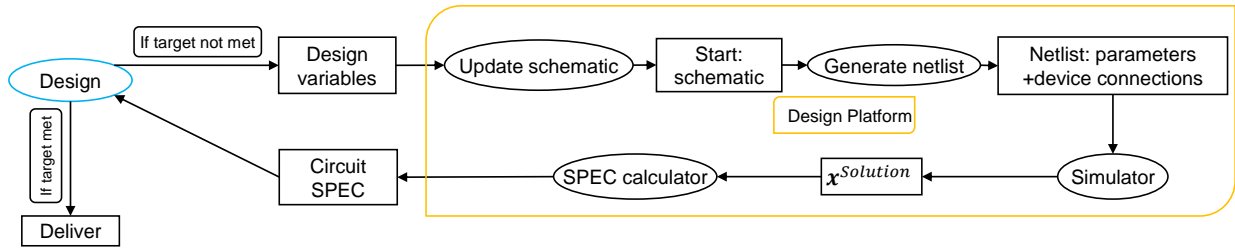


Figure 8: Manual device sizing: an iterative process

This process can be naturally converted into an optimization problem. The optimization strategy varies depending on whether the gradient is acquirable [28–37]. Take DC simulation as an example. To obtain the gradient, the DC steady-state equations  $\mathbf{F}(\mathbf{x}, \mathbf{p}) = \mathbf{0}$  naturally provide an implicit mapping from the parameter  $\mathbf{p}$  to the solution  $\mathbf{x}^{solution}$  of the systems of equations, with the Jacobian matrix of this mapping being  $\nabla_{\mathbf{p}} \mathbf{x}^{solution} = -\nabla_{\mathbf{x}} \mathbf{F} \backslash \nabla_{\mathbf{p}} \mathbf{F}$ , where  $\nabla_{\mathbf{x}} \mathbf{F}$ ,  $\nabla_{\mathbf{p}} \mathbf{F}$  may be directly given by the equations system construction method (computational graph 3b) described in Section 2. With this information, the gradient optimization method (Figure 9) can be used. Note that in an optimization process, the inverse of  $\nabla_{\mathbf{x}} \mathbf{F}$  does not need to be completely solved. Instead, it is sufficient to solve a set of linear equations only once during each iteration's gradient backpropagation for a given loss function or constraint function  $l$ :  $\nabla_{\mathbf{p}} l(\mathbf{x}^{solution}) = (\nabla_{\mathbf{p}} \mathbf{x})^T \cdot \nabla_{\mathbf{x}} l = -(\nabla_{\mathbf{p}} \mathbf{F})^T \cdot (\nabla_{\mathbf{x}} \mathbf{F}^T \backslash \nabla_{\mathbf{x}} l)$

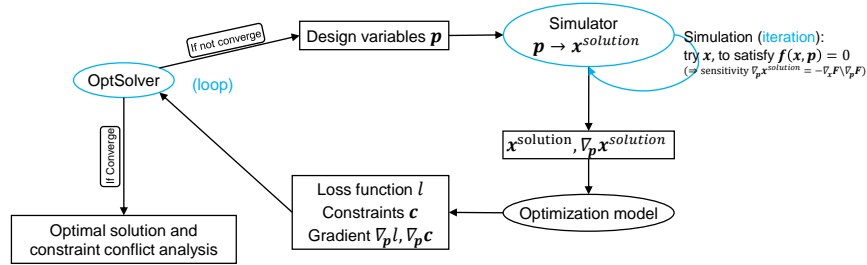
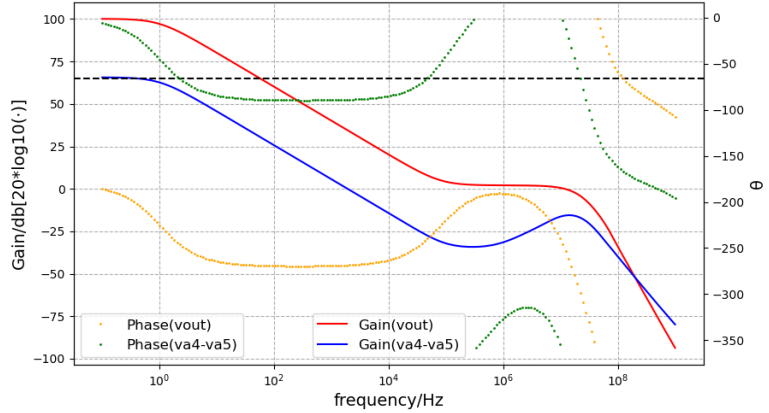
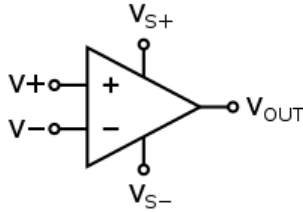


Figure 9: Automatic device sizing

Taking an OpAmp (Figure 10a) as an example, consider the design variables of the circuit (i.e., the channel length and width of each MOSFET) as the variables to be optimized. Given the external current and voltage sources  $I_{bias0}$ ,  $I_{bias1}$ , and  $V_{dd}$ ,  $V_+$ ,  $V_-$  and the load resistance and capacitance  $R_L = 200\Omega$ ,  $C_L = 10^{-10}\text{F}$ , set the optimization goals as follows:

1. The DC operating points of all MOSFETs must be saturated under nine PVT conditions defined by  $Corner \in [tt, ff, ss]$ ,  $Temperature \in [27, -40, 125]$ . For example, for an NMOS, its DC bias voltage must satisfy

$$\min(V_{gs}, V_{ds}, V_{sb}, V_{gs} - V_{th}) \geq 0,$$



(a) OpAmp schematic diagram [53]

(b) Input and output frequency response curves of the OpAmp after sizing

Figure 10: **(a)**: OpAmp schematic diagram, including the bias circuit and the main circuit, and a total of 17 n-MOSFET and 17 p-MOSFET devices. At the DC operating point, when small-signal disturbance with a given frequency is applied at  $V_+$ ,  $V_-$ , an output signal is detected at  $V_{out}$ . **(b)**: Frequency response curves of OpAmp after sizing under  $Corner = tt, Temperature = 27$  conditions, where,  $va4$  and  $va5$  are the two internal nodes in the circuit.

where,  $V_{th}$  is subject to  $MosL, V_{gs}, V_{ds}$ . For different PVT conditions, the SubModel needs to load different databases, and therefore the final simulation solutions obtained are also different.

2. Under the typical condition of  $Corner = tt, Temperature = 27$ , slight fluctuation is allowed for voltage sources  $V_+, V_-$  as long as  $V_+ + V_- = 5v$  is satisfied. For the DC bias of  $V_{out}$ , the maximum must be greater than 4.35 V, and the minimum must be less than 0.3 V. Because our model (Section 3.1) is not used in the TRAN analysis, this requirement plays a similar role as the output swing indicator of circuits.
3. AC analysis is performed on the circuit under the typical condition  $Corner = tt, Temperature = 27$  and a  $v_{in+}, v_{in-} = \pm 0.5$  signal is applied at  $V_+, V_-$ . The DC gain  $gain = 20 \cdot \log_{10}(|v_{out}|)$  of  $V_{out}$  must reach 100.
4. The design variables of each device meet given symmetry constraints. For example, the input MOSFET pair  $M_{n0\_in}, M_{n0\_ip}$  have the same size ( $MosL, MosW$ ), and the current mirrors  $M_{p30\_mirr}, M_{p20\_mirr}, M_{p10\_mirr}, M_{p50\_mirr}, M_{p60\_mirr}$  have the same channel length ( $MosL$ ).

$$\begin{aligned}
 \min_{\mathbf{p}} l &= \max(5 - \log_{10}(|v[out]|), 0)^2 \\
 \text{s. t.} \quad \forall c \in [tt, ff, ss], t \in [27, -40, 125], \\
 &\mathbf{x}_L \preceq \mathbf{x}^{c,t} \preceq \mathbf{x}_U; \text{Saturation}(\mathbf{x}^{c,t}, \mathbf{p}) \succeq \mathbf{0}; \\
 &\mathbf{x}^{down}[out] \leq 0.3; \mathbf{x}^{up}[out] \geq 4.35; \\
 &\mathbf{v} = \mathbf{A}^{tt,27} \backslash \mathbf{b}^{tt,27}; \mathbf{C} \cdot \mathbf{p} = \mathbf{0}.
 \end{aligned} \tag{3}$$

This design task can be expressed as a constrained optimization problem Prob.(3).  $\mathbf{p} \rightarrow \{\mathbf{x}^{c,t}, \mathbf{x}^{down}, \mathbf{x}^{up}\}$  is obtained by solving the system of DC equations under corresponding PVT conditions with input bias  $V_+, V_-$ . And  $\mathbf{v} = \mathbf{A}^{tt,27} \backslash \mathbf{b}^{tt,27} \triangleq \mathbf{A} \backslash \mathbf{b}$  solves the system of AC linear equations under the  $Corner = tt, temperature = 27$  condition, where the matrix elements of  $\mathbf{A}$  are GM, GDS, etc. of each device subject to  $\mathbf{x}^{tt,27}, \mathbf{p}$ . We can use a computational graph of mixed DCAC analysis to calculate  $\mathbf{A}, \mathbf{b}, \nabla_{\mathbf{x}} \mathbf{A}, \nabla_{\mathbf{x}} \mathbf{b}^2$ , which can further enable the calculation of  $\nabla_{\mathbf{x}} l, \nabla_{\mathbf{p}} l$  (Appendix C).  $\mathbf{C} \cdot \mathbf{p} = \mathbf{0}$  represents the direct constraints on design variables, such as a symmetry constraint.

The optimization algorithm is implemented by using the open-source software Ipopt [54] and includes 72 variables, 27 equality constraints, and 308 inequality constraints to be solved. It took 356 seconds to run the whole process (including compiling Julia code and parsing netlist, etc.) on six threads on Intel(R) Core(TM) i7-8700 CPU at 3.20 GHz. Figure 10b shows the frequency response curve of the optimized circuit. The experimental results show that:

<sup>2</sup> $A = i\omega \cdot \nabla_{\mathbf{x}} \mathbf{Q} + \nabla_{\mathbf{x}} \mathbf{F}$ . For a simpler graph implementation, use the DCAC computational graph (instead of  $\nabla \mathbf{Q}, \nabla \mathbf{F}$ ) to calculate  $\nabla \mathbf{A}$ . This avoids calculating and propagating backward the second derivative of  $\mathbf{Q}, \mathbf{F}$  with regard to  $\mathbf{x}$ .

1. In hierarchical circuit simulation or sizing based on the computational graph, the device model and solution algorithm are decoupled from each other, allowing for high flexibility and efficiency.
2. The parameters in the computational graph are processed to function as variables, making gradient optimization of many indicators simpler and easier.

Note that the preceding experiments only consider the operation points of devices and circuit DC gains under typical conditions. To complete the design, more indicators (even discrete value indicators) need to be introduced into the optimization problem. There is no shortcut to properly integrating all indicators into the optimization framework, which however will not be addressed here.

## 4 Conclusion

In this paper, the static parameters of the circuit are processed as runtime variables in simulation, and the structural information and behavioral information of the circuit module/device are decoupled as "equivalent subcircuit decomposition + submodel-computed dynamic parameters". These further derive the computational graph representation of the equations system constructor for hierarchical circuits with circuit modules as the compute units of the computational graph. According to the two simple examples, this approach facilitates the decoupling and flexible interaction between netlists, models, and simulation and optimization algorithms. However, some problems exist with this approach. For example, because the variable gradient will be passed across the layers of a circuit, the topology analysis for circuit equations solvability and DAE-Index no longer works, requiring a more general hierarchical analysis theory. In the future, this approach will gain better generalization by supporting BSIM and more simulation types with more effects (i.e., S parameter or thermal effect) considered. Faster simulation is also possible if the program itself is optimized and the support for fast-SPICE technology is added.

## Acknowledgment

I would like to thank my colleagues at HiSilicon. It's been both a pleasure and an honor to work with them. This work has been also supported by many EDA and HDL experts, including Waisum Wang, Jiewen Fan, Zuochang Ye, Yang Lu, Shangxia Fang, Guoyong Shi, and Yu Ji. Special thanks go to Zhenya Zhou, Jiawei Zhuang, Long Wang, and Yuwei Fan for their kind help.

## References

- [1] Laurence Nagel and Ronald Rohrer. Computer analysis of nonlinear circuits, excluding radiation (CANCER). *IEEE Journal of Solid-State Circuits*, 6(4):166–182, 1971.
- [2] WJ McCalla and WG Howard. BIAS-3-A program for the nonlinear dc analysis of bipolar transistor circuits. *IEEE Journal of Solid-State Circuits*, 6(1):14–19, 1971.
- [3] Laurence W. Nagel and D.O. Pederson. SPICE (Simulation Program with Integrated Circuit Emphasis). Technical Report UCB/ERL M382, EECS Department, University of California, Berkeley, Apr 1973. URL <http://www2.eecs.berkeley.edu/Pubs/TechRpts/1973/22871.html>.
- [4] Diana Estévez Schwarz and Caren Tischendorf. Structural analysis of electric circuits and consequences for MNA. *International Journal of Circuit Theory and Applications*, 28(2):131–162, 2000.
- [5] Peter Kunkel and Volker Mehrmann. *Differential-algebraic equations: analysis and numerical solution*, volume 2. European Mathematical Society, 2006.
- [6] Michael Günther, Uwe Feldmann, and Jan ter Maten. Modelling and discretization of circuit problems. *Handbook of numerical analysis*, 13:523–659, 2005.
- [7] Yogesh Singh Chauhan, Sriram Venugopalan, Mohammed A Karim, Sourabh Khandelwal, Navid Paydavosi, Pankaj Thakur, Ali M Niknejad, and Chenming C Hu. BSIM—Industry standard compact MOSFET models. In *2012 Proceedings of the European Solid-State Device Research Conference (ESSDERC)*, pages 46–49. IEEE, 2012.
- [8] Tatsuya Ezaki, Hans Jurgen Mattausch, and Mitiko Miura-mattausch. *Physics And Modeling Of Mosfets, The: Surface-potential Model Hisim*. World Scientific, 2008.
- [9] Gennady Goldenblat, Xin Li, Weimin Wu, Hailing Wang, Amit Jha, Ronald Van Langevelde, Geert DJ Smit, Andries J Scholten, and Dirk BM Klaassen. PSP: An advanced surface-potential-based MOSFET model for circuit simulation. *IEEE Transactions on Electron Devices*, 53(9):1979–1993, 2006.

- [10] Gary Hachtel, R Brayton, and Fred Gustavson. The sparse tableau approach to network analysis and design. *IEEE Transactions on circuit theory*, 18(1):101–113, 1971.
- [11] Chung-Wen Ho, Albert Ruehli, and Pierce Brennan. The modified nodal approach to network analysis. *IEEE Transactions on circuits and systems*, 22(6):504–509, 1975.
- [12] JG Fijnvandraat, SHMJ Houben, EJW ter Maten, and JMF Peters. Time domain analog circuit simulation. In *International Workshop on Computational codes: Technological Aspects of Mathematics*, 2002.
- [13] Ognen Nastov, Rircardo Telichevesky, Ken Kundert, and Jacob White. Fundamentals of fast simulation algorithms for RF circuits. *Proceedings of the IEEE*, 95(3):600–621, 2007.
- [14] Farid N Najm. *Circuit simulation*. John Wiley & Sons, 2010.
- [15] HDL Verilog. Verilog-AMS Language Reference Manual. *Eda-Stds. Org*, 2014.
- [16] IEEE Standards Association et al. IEEE standard for Verilog hardware description language (IEEE 1364-2005). <http://standards.ieee.org/>, 2006.
- [17] Laurant Lemaitre, Colin McAndrew, and Steve Hamm. ADMS-automatic device model synthesizer. In *Proceedings of the IEEE 2002 Custom Integrated Circuits Conference (Cat. No. 02CH37285)*, pages 27–30. IEEE, 2002.
- [18] Ernst Christen and Kenneth Bakalar. VHDL-AMS-a hardware description language for analog and mixed-signal applications. *IEEE Transactions on Circuits and Systems II: Analog and Digital Signal Processing*, 46(10):1263–1272, 1999.
- [19] François Pêcheux, Christophe Lallement, and Alain Vachoux. VHDL-AMS and Verilog-AMS as alternative hardware description languages for efficient modeling of multidiscipline systems. *IEEE transactions on Computer-Aided design of integrated Circuits and Systems*, 24(2):204–225, 2005.
- [20] Peter BL Meijer. Neural networks for device and circuit modelling. In *Scientific Computing in Electrical Engineering*, pages 251–258. Springer, 2001.
- [21] Lining Zhang and Mansun Chan. Artificial neural network design for compact modeling of generic transistors. *Journal of Computational Electronics*, 16(3):825–832, 2017.
- [22] Moning Zhang, Yang Tang, and Zuochang Ye. Large-signal MOSFET modeling using frequency-domain nonlinear system identification. In *2014 IEEE/ACM International Conference on Computer-Aided Design (ICCAD)*, pages 626–632. IEEE, 2014.
- [23] Zhe Zhang, Runsheng Wang, Cheng Chen, Qianqian Huang, Yangyuan Wang, Cheng Hu, Dehuang Wu, Joddy Wang, and Ru Huang. New-generation design-technology co-optimization (DTCO): Machine-learning assisted modeling framework. In *2019 Silicon Nanoelectronics Workshop (SNW)*, pages 1–2. IEEE, 2019.
- [24] Sitansusekhar Roymohapatra, Ganesh R Gore, Akanksha Yadav, Mahesh B Patil, Krishnan S Rengarajan, Subramanian S Iyer, and Maryam Shojaei Baghini. A novel hierarchical circuit LUT model for SOI technology for rapid prototyping. *IEEE Transactions on Computer-Aided Design of Integrated Circuits and Systems*, 39(5):1073–1083, 2019.
- [25] Behzad Razavi. *Design of analog CMOS integrated circuits*. Tata McGraw-Hill Education, 2002.
- [26] Flandre Silveira, Denis Flandre, and Paul GA Jespers. A  $g_m/I_D$ -based methodology for the design of CMOS analog circuits and its application to the synthesis of a silicon-on-insulator micropower OTA. *IEEE journal of solid-state circuits*, 31(9):1314–1319, 1996.
- [27] Paul Jespers. *The  $g_m/I_D$  Methodology, a sizing tool for low-voltage analog CMOS Circuits: The semi-empirical and compact model approaches*. Springer Science & Business Media, 2009.
- [28] Yong Zhan and Sachin S Sapatnekar. Optimization of integrated spiral inductors using sequential quadratic programming. In *Proceedings Design, Automation and Test in Europe Conference and Exhibition*, volume 1, pages 622–627. IEEE, 2004.
- [29] Bhavna Agrawal, Frank Liu, and Sani Nassif. Circuit optimization using scale based sensitivities. In *IEEE Custom Integrated Circuits Conference 2006*, pages 635–638. IEEE, 2006.
- [30] Guanming Huang, Liuxi Qian, Siwat Saibua, Dian Zhou, and Xuan Zeng. An efficient optimization based method to evaluate the DRV of SRAM cells. *IEEE Transactions on Circuits and Systems I: Regular Papers*, 60(6):1511–1520, 2013.
- [31] Arthur Nieuwoudt and Yehia Massoud. Multi-level approach for integrated spiral inductor optimization. In *Proceedings of the 42nd annual Design Automation Conference*, pages 648–651, 2005.

- [32] Bo Peng, Fan Yang, Changhao Yan, Xuan Zeng, and Dian Zhou. Efficient multiple starting point optimization for automated analog circuit optimization via recycling simulation data. In *2016 Design, Automation & Test in Europe Conference & Exhibition (DATE)*, pages 1417–1422. IEEE, 2016.
- [33] Alessandro Girardi and Lucas C Severo. Analog CMOS Design Automation Methodologies for Low-Power Applications. *Advances in Analog Circuits*, page 1, 2011.
- [34] Wenlong Lyu, Fan Yang, Changhao Yan, Dian Zhou, and Xuan Zeng. Batch Bayesian optimization via multi-objective acquisition ensemble for automated analog circuit design. In *International conference on machine learning*, pages 3306–3314. PMLR, 2018.
- [35] Ye Wang, Michael Orshansky, and Constantine Caramanis. Enabling efficient analog synthesis by coupling sparse regression and polynomial optimization. In *Proceedings of the 51st Annual Design Automation Conference*, pages 1–6, 2014.
- [36] Wenlong Lyu, Pan Xue, Fan Yang, Changhao Yan, Zhiliang Hong, Xuan Zeng, and Dian Zhou. An efficient bayesian optimization approach for automated optimization of analog circuits. *IEEE Transactions on Circuits and Systems I: Regular Papers*, 65(6):1954–1967, 2017.
- [37] Changcheng Tang, Zuochang Ye, and Yan Wang. Parametric circuit optimization with reinforcement learning. In *2018 IEEE Computer Society Annual Symposium on VLSI (ISVLSI)*, pages 197–202. IEEE, 2018.
- [38] A Mahmutoglu, Xufeng Wang, and Jaijeet Roychowdhury. New generation verilog-A model development tools: VAPP and VALint. *New Generation Verilog-A Model Development Tools: VAPP and VALint, Tech. Rep*, 2018.
- [39] Pascal Kuthe, Markus Müller, and Michael Schröter. VerilogAE: An Open Source Verilog-A Compiler for Compact Model Parameter Extraction. *IEEE Journal of the Electron Devices Society*, 8:1416–1423, 2020.
- [40] Wenfei Hu, Zuochang Ye, and Yan Wang. Adjoint transient sensitivity analysis for objective functions associated to many time points. In *2020 57th ACM/IEEE Design Automation Conference (DAC)*, pages 1–6. IEEE, 2020.
- [41] Ian Goodfellow, Yoshua Bengio, and Aaron Courville. *Deep learning*. MIT press, 2016.
- [42] Atilim Gunes Baydin, Barak A Pearlmutter, Alexey Andreyevich Radul, and Jeffrey Mark Siskind. Automatic differentiation in machine learning: a survey. *Journal of Machine Learning Research*, 18:1–43, 2018.
- [43] Linfeng Zhang, Jiequn Han, Han Wang, Roberto Car, and EJPRL Weinan. Deep potential molecular dynamics: a scalable model with the accuracy of quantum mechanics. *Physical review letters*, 120(14):143001, 2018.
- [44] Zichao Long, Yiping Lu, Xianzhong Ma, and Bin Dong. PDE-Net: Learning PDEs from data. In *International Conference on Machine Learning*, pages 3208–3216. PMLR, 2018.
- [45] Zichao Long, Yiping Lu, and Bin Dong. PDE-Net 2.0: Learning PDEs from data with a numeric-symbolic hybrid deep network. *Journal of Computational Physics*, 399:108925, 2019.
- [46] EJW Ter Maten. Numerical methods for frequency domain analysis of electronic circuits. *Survey on Mathematics for Industry*, 8:171–185, 1999.
- [47] Tamal Mukherjee and Gary K Fedder. Hierarchical mixed-domain circuit simulation, synthesis and extraction methodology for MEMS. *Journal of VLSI signal processing systems for signal, image and video technology*, 21(3):233–249, 1999.
- [48] Andrei Tcherniaev, Iouri Feinberg, Walter Chan, Jeh-Fu Tuan, and An-Chang Deng. Transistor level circuit simulator using hierarchical data, June 10 2003. US Patent 6,577,992.
- [49] Jeff Bezanson, Alan Edelman, Stefan Karpinski, and Viral B. Shah. Julia: A fresh approach to numerical computing. *SIAM Review*, 59(1):65–98, 9 2017. doi: 10.1137/141000671.
- [50] Alfred V Aho, Monica S Lam, Ravi Sethi, and Jeffrey D Ullman. *Compilers: principles, techniques, & tools*. Pearson Education India, 2007.
- [51] Steven Muchnick et al. *Advanced compiler design implementation*. Morgan kaufmann, 1997.
- [52] Andrew W Appel. *Modern compiler implementation in C*. Cambridge university press, 2004.
- [53] Wikipedia: Operational Amplifier.
- [54] Andreas Wächter and Lorenz T Biegler. On the implementation of an interior-point filter line-search algorithm for large-scale nonlinear programming. *Mathematical programming*, 106(1):25–57, 2006.

## Appendix

### A TRAN Analysis Induced AC Analysis Equation

To solve the transient equation Eq (Flat) and the DC steady-state equation  $F(\mathbf{x}, \mathbf{p}) = \mathbf{0}$ , the Newton-Raphson method calculates  $\mathbf{Q}, \mathbf{F} \in \mathbb{R}^N$  and the Jacobian matrix  $\nabla_{\mathbf{x}}\mathbf{Q}, \nabla_{\mathbf{x}}\mathbf{F} \in \mathbb{R}^{N \times N}$  repeatedly. In AC small-signal analysis, consider applying perturbation  $\delta\mathbf{x}, \delta\mathbf{p}$  around the steady-state solution  $\mathbf{x}, \mathbf{p}$  and linearizing Eq (Flat) as follows:

$$\nabla_{\mathbf{x}}\mathbf{Q} \cdot \delta\mathbf{x} + \nabla_{\mathbf{p}}\mathbf{Q} \cdot \delta\mathbf{p} + \nabla_{\mathbf{x}}\mathbf{F} \cdot \delta\mathbf{x} + \nabla_{\mathbf{p}}\mathbf{F} \cdot \delta\mathbf{p} = \mathbf{0}$$

Let  $\delta\mathbf{x}, \delta\mathbf{p}$  be a small signal with an angular frequency of  $\omega$ :  $\delta\mathbf{x} = \boldsymbol{\epsilon}_x \cdot e^{i\omega t}, \delta\mathbf{p} = \boldsymbol{\epsilon}_p \cdot e^{i\omega t}$ . Then the system of linear equations of AC small-signal analysis is

$$(i\omega \cdot \nabla_{\mathbf{x}}\mathbf{Q} + \nabla_{\mathbf{x}}\mathbf{F}) \cdot \boldsymbol{\epsilon}_x = (i\omega \cdot \nabla_{\mathbf{p}}\mathbf{Q} + \nabla_{\mathbf{p}}\mathbf{F}) \cdot \boldsymbol{\epsilon}_p \quad (4)$$

### B CMOS Subcircuit

Listing 2: CMOS subcircuit

```
"NMOSTYPE":{
  "ExternalNodes":["gate","source","drain","bulk"],
  "InputParams":["MosL","MosW"],
  "InternalNodes":[],
  "SubModel":{
    "Analysis":["DC","TRAN"],
    "ModelLoader":"SimInfo->lut.MosLookup(\"NMOSTYPE\",
      /path/to/data; SimInfo=SimInfo)",
    "IntrinsicParams":
      ["ID","GDS","CDD","CSS","CGG","CGS","CGD","GM","GMB"]
  },
  "Schematic":{
    "ids":{
      "MasterName":"ICS",
      "ExternalNodes":{"input":"source","output":"drain"},
      "InputParams":{"dc":"ID","ac":0}
    },
    "template":{
      "MasterName":"MosSmallSignalTemplate",
      "ExternalNodes":{
        "gate":"gate","source":"source",
        "drain":"drain","bulk":"bulk"
      },
      "InputParams":{
        "GDS":"GDS","CDD":"CDD","CSS":"CSS","CGG":"CGG",
        "CGS":"CGS","CGD":"CGD","GM":"GM","GMB":"GMB"
      }
    }
  }
}
```

Listing 3: MosSmallSignalTemplate: Small signal equivalent circuit decomposition

```
"MosSmallSignalTemplate":{
  "ExternalNodes":["gate","source","drain","bulk"],
  "InputParams":["GDS","CDD","CSS","CGG","CGS","CGD","GM","GMB"],
  "InternalNodes":[],
  "Schematic":{
    "infr":{
      "MasterName":"resistor",
      "ExternalNodes":{"left":"drain","right":"source"},
    }
  }
}
```



```

    "InputParams": {"resistance": 1e1000}
  },
  "gds": {
    "MasterName": "ACVCCS",
    "ExternalNodes": {"left": "drain", "right": "source", "input": "drain", "output": "source"},
    "InputParams": {"MF": "GDS"}
  },
  "cdd": {
    "MasterName": "capacitor",
    "ExternalNodes": {"input": "drain", "output": "bulk"},
    "InputParams": {"capacitance": "CDD"}
  },
  "css": {
    "MasterName": "capacitor",
    "ExternalNodes": {"input": "source", "output": "bulk"},
    "InputParams": {"capacitance": "CSS"}
  },
  "cgg": {
    "MasterName": "capacitor",
    "ExternalNodes": {"input": "gate", "output": "bulk"},
    "InputParams": {"capacitance": "CGG"}
  },
  "cgs": {
    "MasterName": "capacitor",
    "ExternalNodes": {"input": "gate", "output": "source"},
    "InputParams": {"capacitance": "CGS"}
  },
  "cgd": {
    "MasterName": "capacitor",
    "ExternalNodes": {"input": "gate", "output": "drain"},
    "InputParams": {"capacitance": "CGD"}
  },
  "gm": {
    "MasterName": "ACVCCS",
    "ExternalNodes": {
      "left": "gate", "right": "source", "input": "drain", "output": "source"
    },
    "InputParams": {"MF": "GM"}
  },
  "gmb": {
    "MasterName": "ACVCCS",
    "ExternalNodes": {
      "left": "bulk", "right": "source", "input": "drain", "output": "source"
    },
    "InputParams": {"MF": "GMB"}
  }
}
}
}

```

### C Gradient Backpropagation of the Solution of a Linear Equations System

Consider a system of real linear equations  $\mathbf{A}(\mathbf{x})\mathbf{v} = \mathbf{b}(\mathbf{x})$  with respect to  $\mathbf{v}$ , where  $\mathbf{A}$ ,  $\mathbf{b}$  are nonlinearly dependent on  $\mathbf{x}$  being a sparse matrix/vector, and  $\nabla_{\mathbf{x}}\mathbf{A}$ ,  $\nabla_{\mathbf{x}}\mathbf{b}$  are computable, then  $\mathbf{v}$  will also be nonlinearly dependent on  $\mathbf{x}$ . Differentiating the system of equations yields:

$$(\mathbf{A} + \nabla_{\mathbf{x}}\mathbf{A} \cdot d\mathbf{x}) \cdot (\mathbf{v} + \nabla_{\mathbf{x}}\mathbf{v} \cdot d\mathbf{x}) = \mathbf{b} + \nabla_{\mathbf{x}}\mathbf{b} \cdot d\mathbf{x}$$

When the zeroth and second order terms are dropped, the following equation holds for any  $d\mathbf{x}$

$$\nabla_{\mathbf{x}}\mathbf{A} \cdot d\mathbf{x} \cdot \mathbf{v} + \mathbf{A} \cdot \nabla_{\mathbf{x}}\mathbf{v} \cdot d\mathbf{x} = \nabla_{\mathbf{x}}\mathbf{b} \cdot d\mathbf{x}, \quad (5)$$

Assume a loss function  $l(\mathbf{v})$ , whose gradient  $\nabla_{\mathbf{v}}l$  can be calculated. Backpropagating the gradient to  $\mathbf{x}$  is equivalent to finding the solution of  $\nabla_{\mathbf{x}}l = \nabla_{\mathbf{v}}l \cdot \nabla_{\mathbf{x}}\mathbf{v}$ . In fact, we do not need to actually calculate  $\nabla_{\mathbf{x}}\mathbf{v}$  and store the data, which can be rather dense. According to Equation 5, we have

$$\begin{aligned}\nabla_{\mathbf{x}}\mathbf{v} \cdot d\mathbf{x} &= \mathbf{A}^{-1} \cdot (\nabla_{\mathbf{x}}\mathbf{b} \cdot d\mathbf{x} - \nabla_{\mathbf{x}}\mathbf{A} \cdot d\mathbf{x} \cdot \mathbf{v}), \forall d\mathbf{x}, \\ \Rightarrow \nabla_{\mathbf{v}}l \cdot \nabla_{\mathbf{x}}\mathbf{v} \cdot d\mathbf{x} &= (\nabla_{\mathbf{v}}l \cdot \mathbf{A}^{-1}) \cdot (\nabla_{\mathbf{x}}\mathbf{b} \cdot d\mathbf{x} - \nabla_{\mathbf{x}}\mathbf{A} \cdot d\mathbf{x} \cdot \mathbf{v}), \forall d\mathbf{x},\end{aligned}$$

Therefore, in order to calculate  $\nabla_{\mathbf{v}}l \cdot \nabla_{\mathbf{x}}\mathbf{v}$ , we only need to solve the sparse matrix linear equations system  $\nabla_{\mathbf{v}}l \cdot \mathbf{A}^{-1}$  once in advance, element-wisely set the values of  $d\mathbf{x}$  to 1 and the rest to 0. Then, we obtain  $\nabla_{\mathbf{x}}l = \nabla_{\mathbf{v}}l \cdot \nabla_{\mathbf{x}}\mathbf{v}$ .

For the case of a set of complex linear equations, a similar discussion can also be carried out using the Wirtinger derivative.